Diagn Interv Radiol 2026; DOI: 10.4274/dir.2026.263576

CARDIOVASCULAR IMAGING

PICTORIAL ESSAY

The imaging spectrum of myocardial infarction and its associated complications: a contemporary pictorial review of computed tomography and magnetic resonance imaging

Yu Zhang[1]
Sung Min Ko[2]

[1]Yuhuangding Hospital, Clinic of Radiology, Yantai, China

[2]Wonju Severance Christian Hospital, Yonsei University Wonju Faculty of Medicine, Department of Radiology, Wonju, South Korea

ABSTRACT

Myocardial infarction (MI) is a leading cause of morbidity and mortality worldwide. Although rapid diagnosis and reperfusion in the acute setting rely primarily on clinical assessment, electrocardiography, echocardiography, and invasive coronary angiography, advanced cardiac imaging plays an essential role beyond the hyperacute phase. Cardiac computed tomography (CCT) and cardiac magnetic resonance (CMR) imaging provide complementary information that extends from coronary anatomy to myocardial tissue characterization and functional assessment. CMR imaging enables the comprehensive, multiparametric evaluation of MI, including left ventricular function, myocardial edema and area at risk, infarct size and transmural extent, microvascular obstruction, intramyocardial hemorrhage, myocardial viability, and ischemia using cine imaging, T1/T2 and T2* mapping, perfusion imaging, and late gadolinium enhancement. These features support an accurate differentiation between acute and chronic infarction, an assessment of myocardial salvage, and prognostic stratification. CCT offers a rapid, non-invasive assessment of coronary artery stenosis and plaque characteristics and has expanded to include an evaluation of ventricular function, myocardial perfusion, and delayed-enhancement patterns. When combined with CT-derived fractional flow reserve or myocardial perfusion imaging, CT allows for an integrated anatomic and functional assessment of the myocardium, particularly for non-culprit lesions, following MI. Myocardial delayed-enhancement CT can visualize the infarcted myocardium and microvascular injury in select patients, though it remains complementary to magnetic resonance imaging. This pictorial essay illustrates the imaging spectrum of MI and its major mechanical and thromboembolic complications, including ventricular rupture, septal defects, papillary muscle rupture, aneurysm formation, left ventricular thrombi, and pericardial disease. By highlighting the strengths and limitations of CCT and CMR and providing practical guidance for modality selection, this article aims to support informed clinical decision-making in the contemporary management of patients with MI.

KEYWORDS

Myocardial infarction, magnetic resonance imaging, computed tomography, delayed enhancement, viability, mapping, microvascular obstruction

Handling editor: Furkan Ufuk

Corresponding author: Sung Min Ko

E-mail: ksm9723@yahoo.co.kr

Received 10 November 2025; revision requested 08 December 2025; accepted 01 February 2026.

Epub: 26.02.2026

Publication date: 01.07.2026

DOI: 10.4274/dir.2026.263576

Myocardial infarction (MI) is a leading cause of morbidity and mortality worldwide.[1] Although rapid reperfusion strategies rely primarily on clinical assessment, electrocardiography (ECG), echocardiography, and invasive coronary angiography, advanced cardiac imaging plays a pivotal role beyond the hyperacute phase. In particular, cardiac magnetic resonance (CMR) imaging and cardiac computed tomography (CCT) provide complementary anatomical, functional, and tissue-level information that informs prognosis, risk stratification, and management after MI. CMR imaging is the reference standard for myocardial tissue characterization, allowing for a multiparametric evaluation of ventricular function, infarct size, myocardial edema, microvascular injury, intramyocardial hemorrhage, and myocardial viability. CCT, which has traditionally focused on coronary anatomy, has evolved to enable functional assessment using CT-derived fractional flow reserve CT myocardial perfusion imaging (CT-MPI), and myocardial delayed-enhancement CT (MDE-CT).[2,3] Recent ad-

You may cite this article as: Zhang Y, Ko SM. The imaging spectrum of myocardial infarction and its associated complications: a contemporary pictorial review of computed tomography and magnetic resonance imaging. *Diagn Interv Radiol*. 2026;32(4):426-436.

vances incorporating artificial intelligence (AI)-based noise suppression and automated infarct segmentation have further expanded the capabilities of CT while reducing radiation exposure.[4] This pictorial essay reviews the imaging spectrum of MI and its complications, emphasizing quantitative biomarkers, modality-specific strengths and limitations, and practical guidance for selecting CCT, CMR imaging, or echocardiography in common clinical scenarios.

Main points

- Myocardial infarction (MI) remains a leading cause of morbidity and mortality worldwide.
- Cardiac magnetic resonance (CMR) imaging enables a detailed evaluation of ventricular function, myocardial viability, area at risk, microvascular obstruction, and intramyocardial hemorrhage through multiparametric imaging.
- Cardiac computed tomography (CCT) allows a rapid, non-invasive assessment of coronary stenosis, myocardial damage, and post-MI complications, aiding prompt clinical decisions.
- Together, CCT and CMR imaging play complementary roles in comprehensive MI evaluation, guiding risk stratification and personalized management.

Overview of myocardial infarction

MI is commonly classified according to the extent of myocardial involvement as either transmural or subendocardial infarction and by its electrocardiographic presentation as either ST-segment elevation MI (STEMI) or non-STEMI.[5] In the setting of prolonged but incomplete ischemia, the myocardium may exhibit reversible contractile dysfunction despite the preservation of myocardial viability, retaining the potential for functional recovery after reperfusion. Accordingly, timely revascularization is critical to limiting irreversible myocardial injury, preserving viable myocardial tissue, and improving clinical outcomes.[6]

Cardiac magnetic resonance imaging

Multiparametric cardiac magnetic resonance imaging protocols

CMR imaging enables a comprehensive evaluation of MI through a multiparametric approach. Standard protocols integrate cine imaging to assess global and regional left ventricular (LV) function; T2-weighted imaging (T2WI) and T2 mapping for myocardial edema and area at risk (AAR); native T1 mapping and extracellular volume (ECV) quantification for diffuse myocardial injury; first-pass perfusion imaging for microvascular integrity; late gadolinium enhancement (LGE) for infarct size, transmural extent, and microvascular obstruction (MVO); and T2* mapping for intramyocardial hemorrhage (IMH). This integrated examination allows for the simultaneous assessment of myocardial injury and salvage and prognostic markers in a single session (Figure 1).[7]

Quantitative cardiac magnetic resonance imaging biomarkers and prognostic implications

Quantitative CMR imaging biomarkers provide clinically relevant prognostic information beyond a visual assessment. Elevated native T1 values (e.g., > 1,250 ms at 1.5 T) and an increased ECV (> 30%) have been associated with adverse LV remodeling. MVO, visualized as a non-enhancing region within the infarcted myocardium, is a strong predictor of poor outcome, with an MVO burden exceeding approximately 1.4% of the LV mass linked to an increased risk of heart failure and major adverse cardiovascular events (MACE) (Figure 2). Moreover, T2* values below 20 ms indicate an IMH and are associated with unfavorable remodeling (Figure 3).[8-10] Texture analysis and radiomics applied to LGE and mapping images have shown promise for predicting LV remodeling and MACE, though these techniques remain investigational.[11]

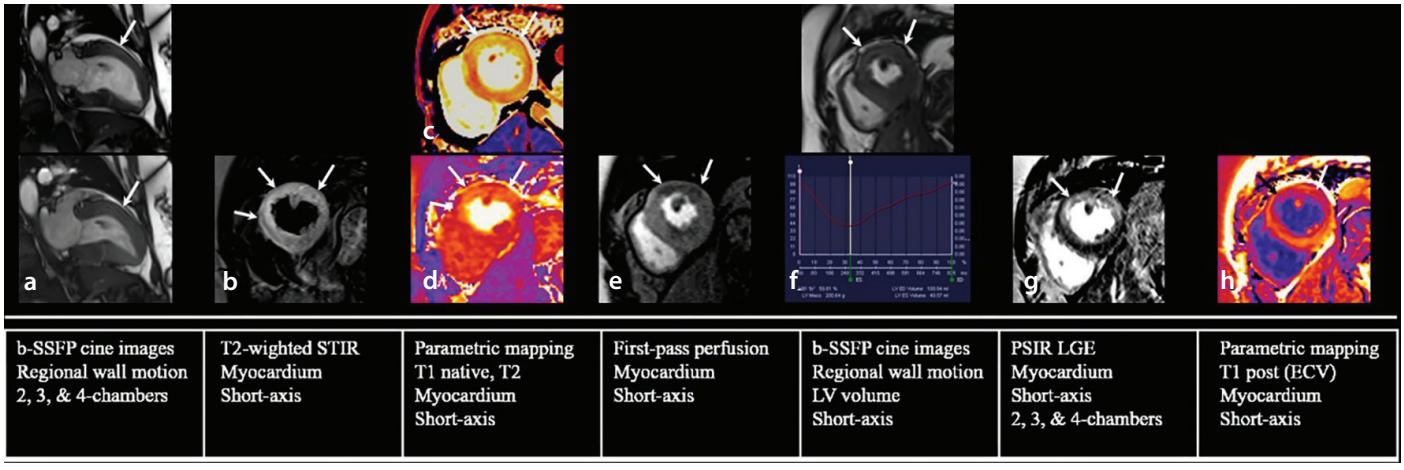

Figure 1. Schematic of the cardiac magnetic resonance protocol workflow in a 65-year-old man with reperfused STEMI. (**a**): Two-chamber b-SSFP cine images at end diastole (upper) and end systole (lower) demonstrate hypokinesia of the mid-anterior left ventricular (LV) segment (arrow). (**b**): T2-weighted STIR image shows transmural high signal intensity consistent with infarct-related myocardial edema in mid-anterior, anteroseptal, and anterolateral LV segments (arrows). (**c, d**): Native T1 (c, upper) and T2 (d, lower) mapping images demonstrate elevated T1 (1,590–1,620 ms) and T2 (62–71 ms) values in the same LV segments (arrows). (**e**): First-pass perfusion image using TurboFLASH shows transmural perfusion defects in mid-anterior and anterolateral LV segments (arrows). (**f**): Quantitative assessment of global LV function on short-axis b-SSFP cine images shows normal LV end-diastolic and end-systolic volumes (101 and 40.6 mL) and a preserved LV ejection fraction of 59.8%. Regional hypokinesia is noted in the mid-anterior and anterolateral segments on the systolic short-axis image (arrows). (**g**): Late gadolinium enhancement image with PSIR demonstrates transmural delayed enhancement in LAD and LCX territories (arrows). (**h**): Post-contrast T1 mapping image shows reduced T1 values (325–360 ms) in the same LV segments as on native T1 mapping (arrows). STEMI, ST-segment elevation myocardial infarction; b-SSFP, balanced steady state-free precession; ECV, extracellular volume; STIR, short tau inversion recovery; FLASH, fast low-angle shot; PSIR, phase-sensitive inversion recovery; LAD, left anterior descending coronary artery; LCX, left circumflex coronary artery.

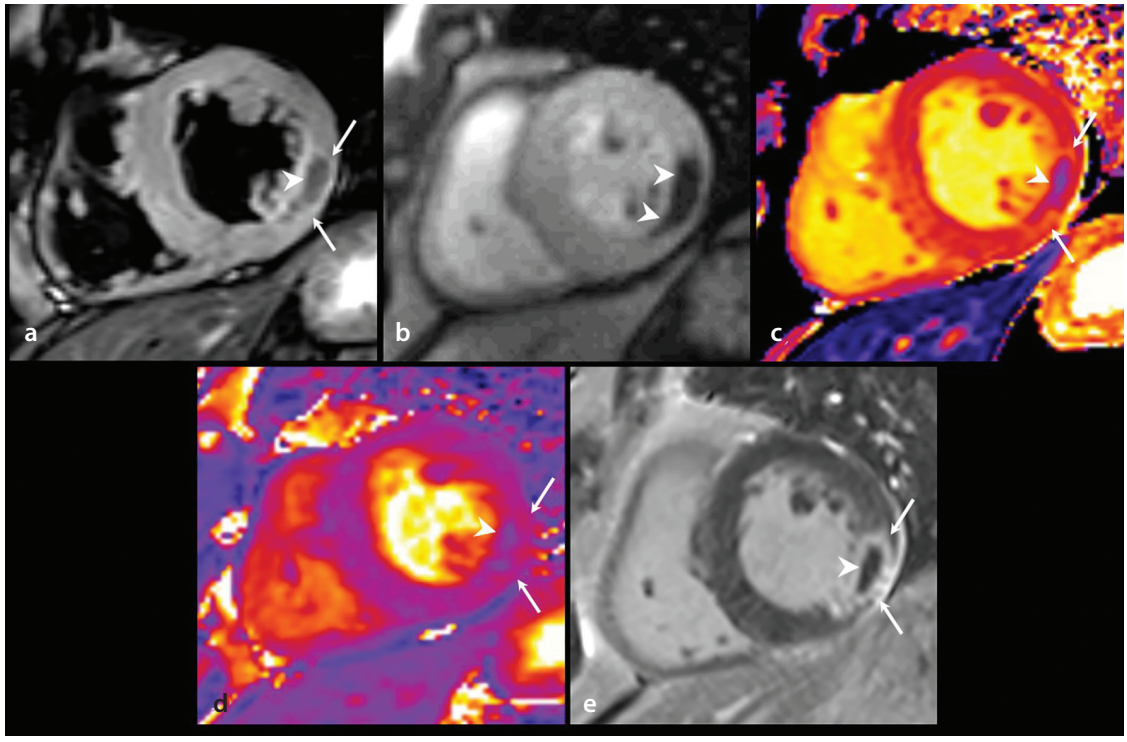

Figure 2. Evaluation of MVO in a 49-year-old man with reperfused STEMI using various CMR imaging techniques (**a**): Short-axis T2-weighted STIR image shows transmural high signal intensity (arrows) and transmural dark signal intensity (arrowhead) in the mid-inferolateral LV segment. (**b**): Short-axis first-pass perfusion image shows a transmural perfusion defect (arrowheads) in the mid-inferolateral LV segment. (**c, d**): Short-axis T1 (**c**) and T2 mapping (**d**) images show elevated T1 (1,379–1,435 ms) and T2 (46–54 ms) values along the infarct border (arrows) and shortened T1 (1,093–1,127 ms, c) and T2 values (27–33 ms, d) in the infarct core (arrowheads). (**e**): Short-axis LGE image shows transmural inferolateral infarction (arrows) with MVO in the infarct core (arrowhead). CMR, cardiac magnetic resonance; MVO, microvascular occlusion; STEMI, ST-segment elevation myocardial infarction; LV, left ventricular; LGE, late gadolinium enhancement; STIR, short tau inversion recovery.

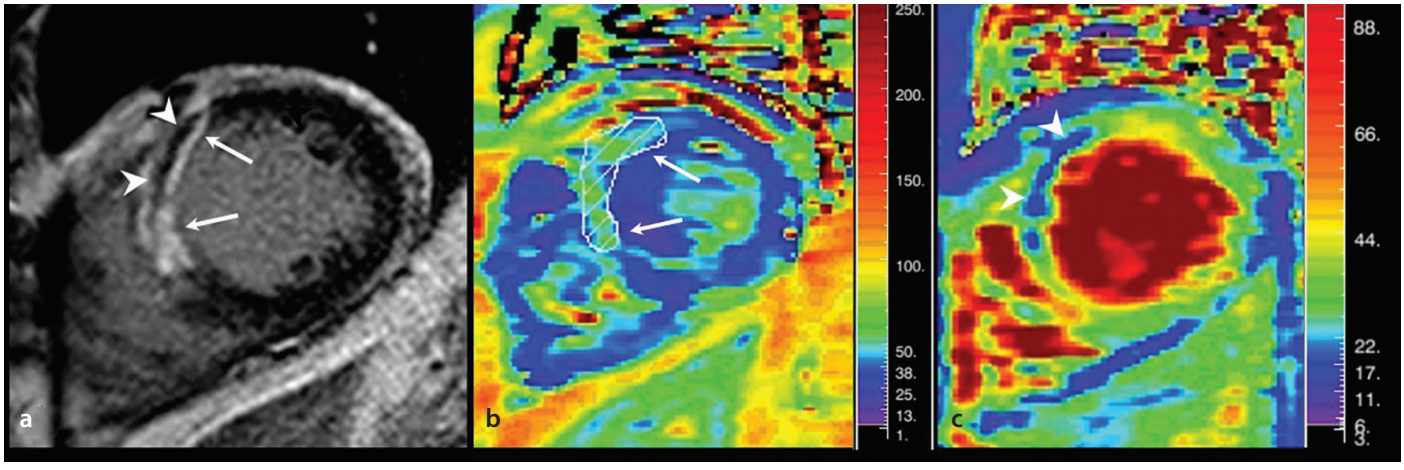

Figure 3. Intramyocardial hemorrhage in a 56-year-old man with acute MI. (**a**): Short-axis LGE image shows mid-anterior and anteroseptal infarction (arrows) with MVO in the infarct core (arrowheads). (**b**): Short-axis T2 mapping image shows lower T2 values (38–42 ms) in the mid-anteroseptal and anterior LV wall (arrows) than in the remote myocardium (50–58 ms). (**c**): Short-axis T2* mapping image shows a shorter T2* time (< 20 ms) in the infarct core (arrowheads), indicating IMH. Photographs courtesy of Jung Im Jung, MD, Department of Radiology, Seoul St. Mary's Hospital, College of Medicine, The Catholic University of Korea. MI, myocardial infarction; IMH, intramyocardial hemorrhage; LGE, late gadolinium enhancement; MVO, microvascular occlusion; LV, left ventricular.

Myocardial viability, ischemia, and stress cardiac magnetic resonance imaging

LGE-CMR imaging remains the reference standard for the assessment of myocardial viability. Segments with < 25% of LGE involvement demonstrate a high likelihood of functional recovery, whereas those with > 75% involvement rarely recover.[12] Stress CMR imaging, and particularly adenosine stress perfusion imaging, enables a robust functional assessment of myocardial ischemia and may be useful for evaluating residual ischemia and non-culprit lesions after MI,[13] and T2 mapping and T2WI help differentiate acute from chronic MI by depicting infarct-related myocardial edema (Figure 4).

Area at risk and myocardial salvage

A primary goal in MI management is to limit infarct size and preserve the AAR. In acute MI, T2WI displays myocardial edema that typically extends beyond the infarct core identified on LGE, with the difference representing salvageable myocardium (Figure 5). Furthermore, T1 and T2 mapping en-

able quantitative assessment of the AAR and myocardial salvage, thus reducing observer dependency and improving reproducibility. A greater myocardial salvage index has been associated with favorable LV remodeling and functional recovery, highlighting the clinical relevance of mapping-based assessment in post-infarction risk stratification and therapeutic decision making.[7,12]

Differentiation between microvascular obstruction, intramyocardial hemorrhage, and myocardial dissecting hematoma

CMR imaging plays a critical role in differentiating between MVO, IMH, and myocardial dissecting hematomas, and accurate distinction between them directly influences their management. MVO appears as a non-enhancing area within the hyperenhanced, infarcted myocardium on LGE and is best delineated on first-pass perfusion imaging. IMH typically co-localizes with MVO and is characterized by shortened T2* values (< 20 ms) resulting from hemosiderin deposition (Figures 2 and 3).[7] By contrast, a myocardial dissecting hematoma presents as an intramyocardial cavity with variable signal intensity, a preserved epicardial contour, and a lack of typical infarct-related enhancement, allowing for its differentiation from reperfusion-related injury and thus guiding appropriate clinical management.[14]

Cardiac computed tomography

Coronary CT angiography (CCTA) allows for a rapid, non-invasive evaluation of coronary stenosis and plaque morphology, including high-risk features associated with acute coronary syndromes (Figure 6). When integrated with CCTA, CT-MPI enables combined anatomic and functional assessment and may be useful for evaluating residual ischemia and non-culprit lesions after MI treated with percutaneous coronary intervention.[15] Dynamic stress and rest CT-MPI examinations enable a quantitative assessment of myocardial blood flow and coronary flow reserve, with reduced coronary flow reserve values (typically < 2.0) commonly used as a marker of myocardial ischemia (Figure 7).[16]

MDE-CT visualizes the infarcted myocardium as delayed iodine enhancement and may identify non-enhancing regions consistent with MVO. Compared with LGE-CMR, MDE-CT has inherent limitations, including a lower contrast-to-noise ratio, greater radiation exposure, a lack of standardized acquisition protocols, and limited availability. Accordingly, MDE-CT should be regarded as a complementary and largely investigational technique that is primarily considered when CMR imaging is contraindicated or when a CT scan is already being performed for coronary assessment (Figure 8). An MDE-CT image is typically acquired 5–10 minutes after contrast administration using low-kV, ECG-triggered delayed scanning with or without a minimal, additional contrast injection.[17] Recent technical advances, including dual-energy iodine mapping and iterative reconstruction, have improved contrast and image quality. In addition, AI-based deep learning denoising enables automated infarct segmentation, enhances the visualization capabilities of MDE, and may facilitate an acceptable image quality at lower radiation doses (Figure 9).[18]

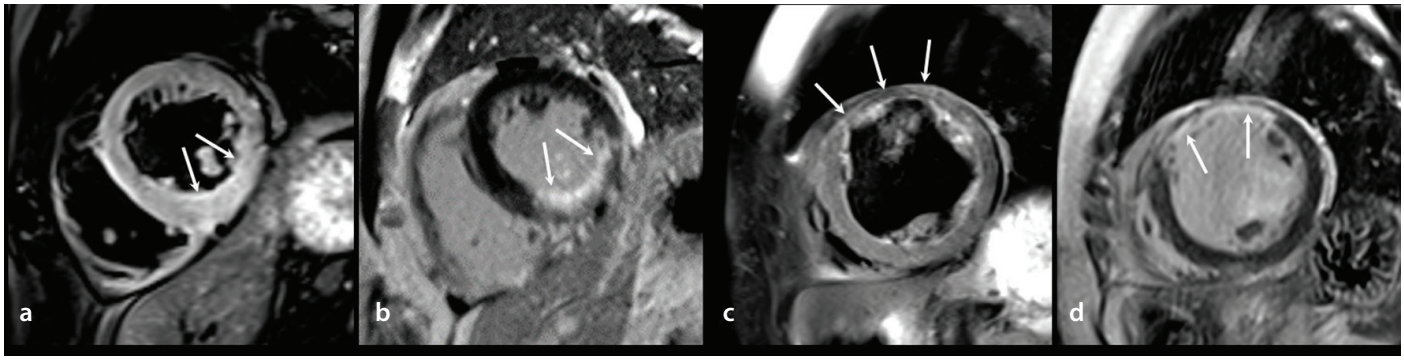

Figure 4. Difference in CMR imaging findings between acute and chronic MI. (**a, b**): Short-axis T2-weighted STIR (**a**) and LGE (**b**) images show transmural high signal intensity (**a**) and delayed enhancement (**b**) in the mid-inferior and inferoseptal LV segments without myocardial thinning (arrows), consistent with acute MI. (**c, d**): Short-axis T2-weighted STIR (**c**) and LGE (**d**) images show a normal T2 signal with myocardial thinning (**c**) and transmural delayed enhancement (**d**) in the mid-anterior LV segment (arrows), consistent with chronic MI. Although T2-weighted STIR alone cannot reliably distinguish acute from chronic MI, the combination of LGE and T2-weighted STIR enables the identification of infarct-related myocardial edema indicative of acute MI. CMR, cardiac magnetic resonance; MI, myocardial infarction; LV, left ventricular; LGE, late gadolinium enhancement; STIR, short tau inversion recovery.

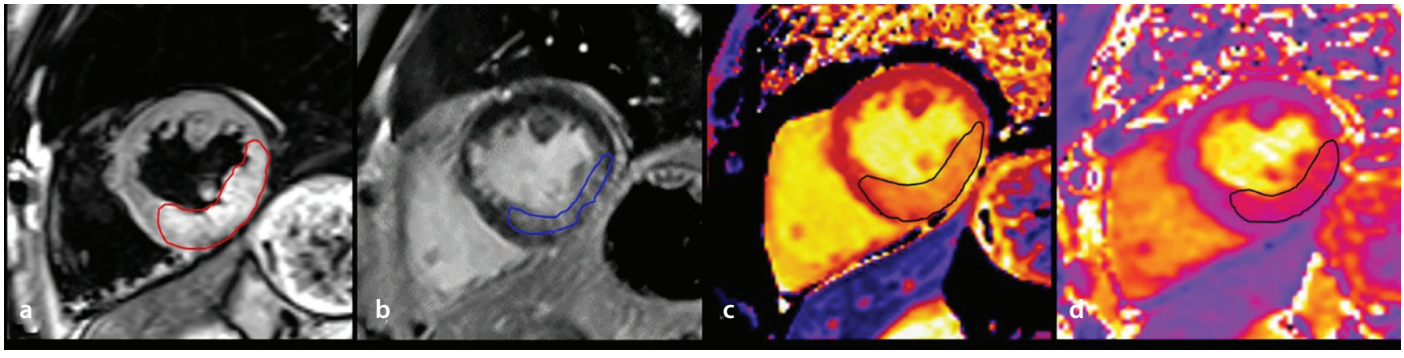

Figure 5. Evaluation of myocardial salvage in a 62-year-old man with reperfused STEMI using T2-weighted STIR and LGE. (**a, b**): Short-axis T2-weighted STIR (**a**) and LGE (**b**) images show transmural high signal intensity (red circle, **a**) and delayed enhancement (blue circle, **b**) in the mid-inferior and inferoseptal LV segments. Myocardial salvage is defined as the hyperintense area on T2-weighted STIR minus infarct size on LGE. (**c, d**): The region of elevated T1 values (1,479–1,535 ms; black circle, (**c**) corresponds to the T2-weighted STIR hyperintense area (**a**) and is larger than the regions of elevated T2 values (50–56 ms; black circle, **d**) and LGE (**b**). STEMI, ST-segment elevation myocardial infarction; LV, left ventricular; LGE, late gadolinium enhancement; STIR, short tau inversion recovery.

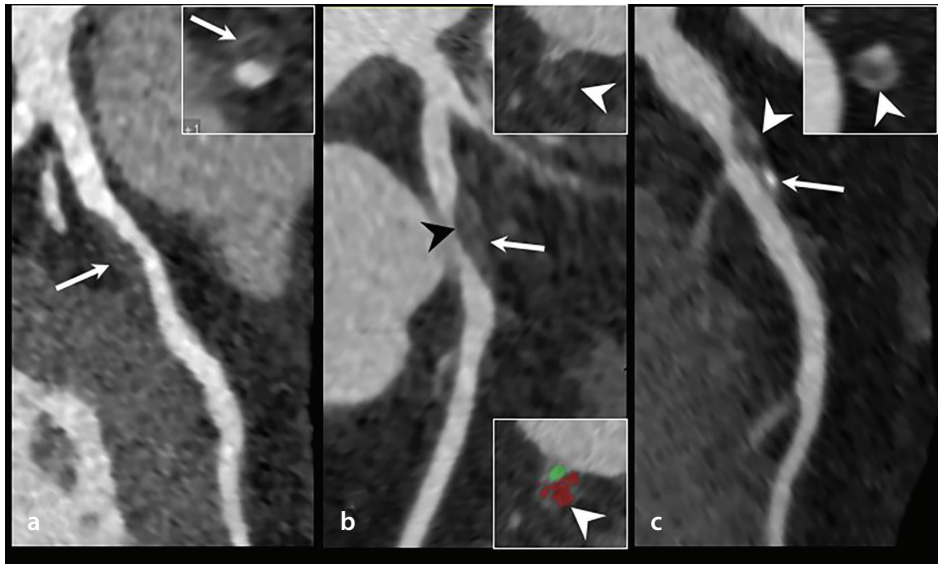

Figure 6. Analysis of vulnerable atherosclerotic plaques using coronary computed tomography angiography. High-risk (vulnerable) plaque features are classified as (**a**) positive remodeling (arrow); (**b**) positive remodeling with low-attenuation plaque (arrowhead); and (**c**) positive remodeling with spotty calcification (arrow) and low-attenuation plaque with a napkin-ring sign (non-calcified plaque with an enhancing ring, arrowhead).

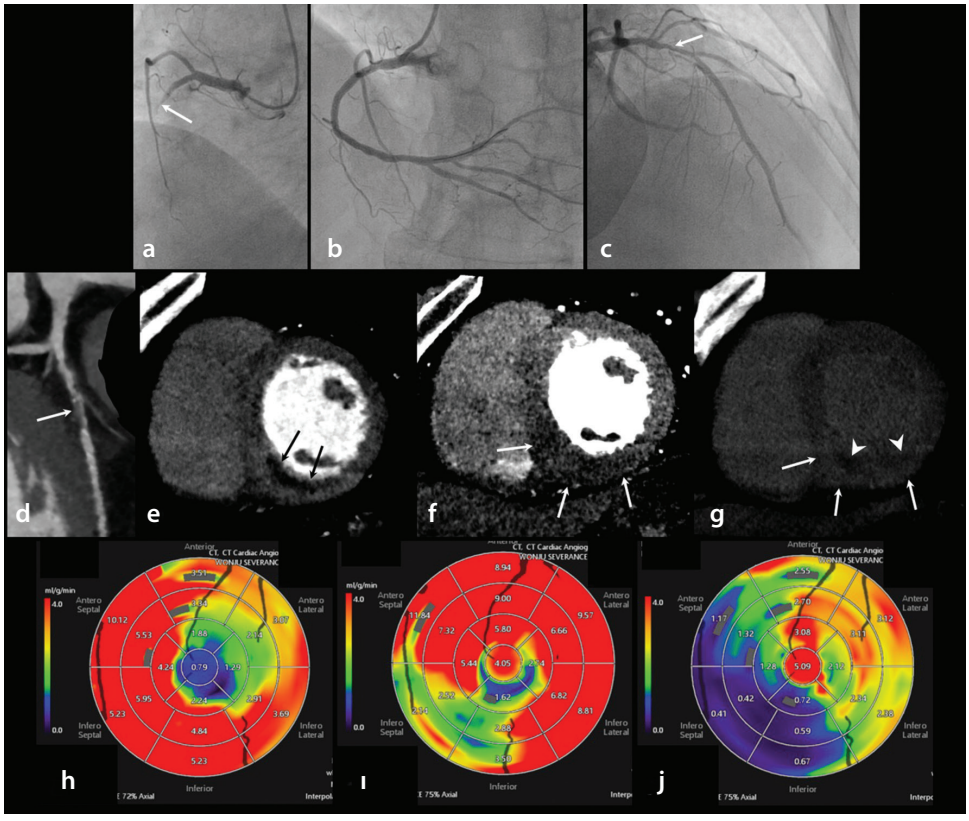

Figure 7. Dynamic CT-MPI to assess the hemodynamic significance of non-infarct-related arteries in reperfused STEMI. (**a–c**): Invasive coronary angiography shows complete thrombotic occlusion of the proximal RCA (**a**, arrow), successfully treated with PCI (**b**). A non-culprit lesion with approximately 70% luminal narrowing is noted in the proximal LAD (**c**, arrow). (**d**): Curved MPR CCTA image shows significant (> 70%) stenosis with non-calcified plaque in the proximal LAD (arrow). (**e, f**): Dynamic stress (**e**) and rest (**f**) CT-MPI shows more pronounced perfusion defects during stress than at rest in the mid-inferior and inferoseptal LV segments (arrows), with no perfusion defects in the LAD territory. (**g**): Myocardial delayed-enhancement short-axis MPR CT image demonstrates transmural delayed enhancement (arrows) with subendocardial non-enhancing areas consistent with MVO (arrowheads) in the RCA territory, indicating acute transmural MI. (**h–j**): Polar maps of dynamic stress (**h**) and rest (**i**) CT-MPI examinations and CFR (**j**). Per-segment CFR_{CT} is calculated as the ratio of hyperemic MBF_{CT} to resting MBF_{CT}. A CFR_{CT} image of the anteroseptal LV wall is reduced (< 1.4) compared with the lateral LV wall (> 2.0). Using the optimal CFRCT cut-off value of 2.0, ischemia is seen in the LAD territory. Invasive FFR was 0.75 in the proximal LAD. Staged physiology-guided PCI was performed on the proximal LAD, and the FFR was increased to 0.91 (not shown). CT, computed tomography; MPI, myocardial perfusion imaging; STEMI, ST-segment elevation myocardial infarction; MPR, multiplanar reformation; LV, left ventricular; CCTA, coronary CT angiography; RCA, right coronary artery; LAD, left anterior descending coronary artery; PCI, percutaneous coronary intervention; MVO, microvascular obstruction; CFR, coronary flow reserve; MBF, myocardial blood flow; FFR, fractional flow reserve.

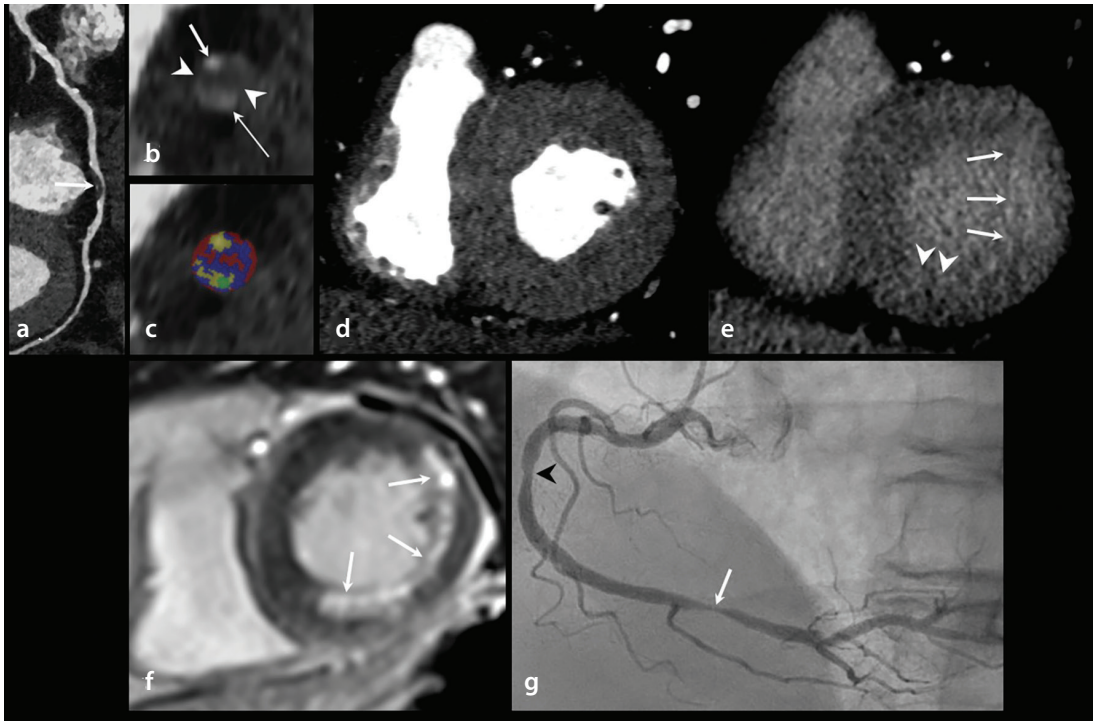

Figure 8. Comprehensive coronary CT angiography assessment of acute MI in a 62-year-old man with NSTEMI. (**a**): Curved multiplanar reformation image of the RCA shows mixed calcified and non-calcified plaques with positive remodeling in the distal RCA (arrow). (**b, c**): Cross-sectional images demonstrate very low-attenuation non-calcified plaque (mean attenuation: 2 ± 34 HU, arrowheads) adjacent to calcified plaque (arrow) and contrast-enhanced lumen (long, thin arrow) (**b**). In acute MI, this finding suggests high-risk plaque with a possible superimposed thrombus, though CT-based differentiation is limited. Quantitative plaque analysis software (**c**) depicts soft (red), fibrous (blue), and calcified (yellow) plaque components. (**d, e**): Early- and delayed-phase short-axis CT images show no early hypoenhancement (**d**), but delayed transmural hyperenhancement (arrows) in the basal lateral LV and subendocardial hyperenhancement (arrowheads) in the inferior LV segments (**e**) are visible, consistent with acute MI. (**f**): Delayed-enhancement CMR image confirms corresponding myocardial enhancement patterns (arrows). (**g**): Invasive coronary angiography shows 80% stenosis in the distal RCA (arrow) and 50% stenosis in the mid-RCA (arrowhead), with a hyperdominant RCA supplying the lateral LV wall. NSTEMI, non-ST-segment elevation myocardial infarction; CT, computed tomography; RCA, right coronary artery; LV, left ventricular; CMR, cardiac magnetic resonance; HU, Hounsfield unit.

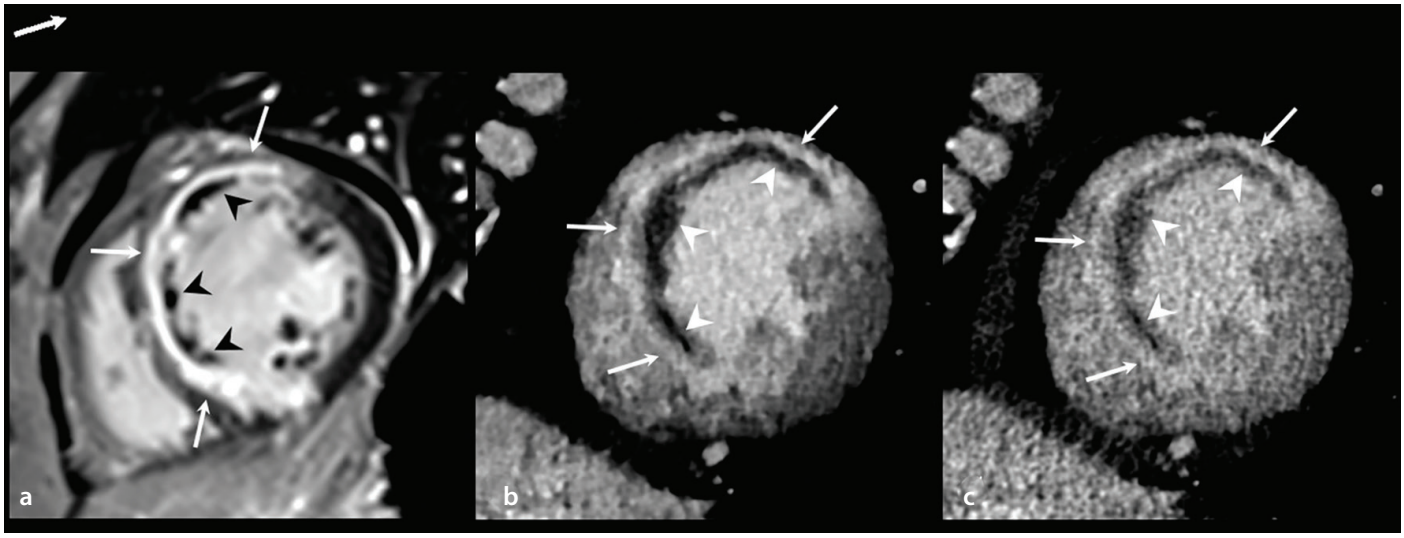

Figure 9. Short-axis MDE-CT images of a 64-year-old man with reperfused STEMI. (**a**): Short-axis LGE-CMR image demonstrates transmural delayed enhancement (arrows) with central non-enhancing areas consistent with MVO (arrowheads) involving the mid-anterior, anterolateral, anteroseptal, and inferoseptal LV segments. (**b, c**): Artificial intelligence-based, contrast-enhanced, and denoised CT image (**b**) shows reduced image noise and improved visualization of transmural delayed enhancement (arrows) and non-enhancing regions consistent with MVO (arrowheads) compared with the standard CT image (**c**). MDE, myocardial delayed enhancement; CT, computed tomography; STEMI, ST-segment elevation myocardial infarction; CMR, cardiac magnetic resonance; LV, left ventricular; LGE, late gadolinium enhancement; MVO, microvascular obstruction; AI, artificial intelligence.

Despite these advances, further external validation and protocol standardization are required before broader clinical adoption can proceed.

Imaging of post-myocardial infarction complications

A variety of mechanical and thromboembolic complications may occur after MI, particularly with delayed or inadequate reperfusion, and are associated with hemodynamic instability and adverse outcomes.[19,20]

Free wall rupture is a catastrophic complication of STEMI. CCT enables rapid assessment, displaying hemopericardium, pericardial effusion, and rupture tracts, whereas LGE-CMR confirms myocardial discontinuity, irregular margins, and associated thrombi, facilitating prompt diagnosis and management (Figure 10).

Ventricular septal rupture is an uncommon but life-threatening complication of MI. CCT provides the rapid, non-invasive detection of septal defects, whereas CMR imaging offers a detailed evaluation of defect size and location and surrounding myocardial integrity, which is essential for surgical planning and prognostic assessment (Figure 11).

Papillary muscle rupture results in acute, severe mitral regurgitation. Echocardiography remains the first-line modality for hemodynamic assessment, whereas CCT and CMR imaging allow for the visualization of papillary muscle integrity and global LV function. In chronic mitral regurgitation, CMR imaging enables an accurate quantification of regurgitant volume and an assessment of myocardial fibrosis using LGE and T1 mapping (Figure 12).

Differentiation between a true aneurysm and a pseudoaneurysm relies heavily on imaging. CCT and CMR imaging assess wall continuity, neck morphology, thrombus formation, and pericardial involvement, which are critical for guiding management decisions (Figures 13 and 14).

LV thrombi are a common post-MI complication. On LGE-CMR, a thrombus appears as a non-enhanced filling defect, with long inversion time imaging improving thrombus conspicuity by suppressing myocardial and blood pool signals. Cine imaging allows for the assessment of thrombus mobility, which aids risk stratification and anticoagulation planning (Figure 13).

Pericardial complications, including pericarditis and effusion, are readily evaluated with CCT for anatomic assessment. CMR imaging enables characterization of pericardial inflammation and enhancement. Fat-suppressed LGE imaging improves visualization of pericardial inflammation by suppressing the adjacent epicardial fat signal, thereby facilitating differentiation between simple effusion and inflammatory pericarditis (Figure 15).

Heart failure represents a major long-term consequence of MI. CMR imaging enables a comprehensive evaluation of ventricular function, valvular mechanics, and myocardial tissue characteristics to support longitudinal assessment and management.

Clinical integration and modality selection

Rather than competing modalities, CCT, CMR imaging, and echocardiography provide synergistic information.[14,16,19,20] Modality selection should be guided by the clinical question at hand, patient stability, contraindications, and local expertise. A practical clinical algorithm summarizing modality choice is provided in Table 1.

Ethics and consent

This pictorial essay was conducted in accordance with institutional ethics standards. Formal institutional review board approval and informed consent were waived owing to the essay's retrospective use of anonymized data.

This pictorial essay does not provide pooled diagnostic accuracy metrics, and quantitative thresholds may vary by scanner, field strength, and post-processing procedures. Advanced CT techniques, such as MDE-CT and CT-MPI, and emerging AI-based and radiomics approaches are not yet widely standardized—a circumstance that could potentially limit the generalizability of this essay's conclusions. Therefore, this article focuses on established and clinically applicable imaging findings.

CCT and CMR imaging provide complementary information in the evaluation of MI beyond the acute phase. CMR imaging enables detailed tissue characterization, viability assessment, and evaluation of post-infarction complications. CCT allows for rapid coronary assessment and functional evaluation and plays an important role in assessing select post-infarction complications. Integrated with echocardiography and clinical context, multimodality imaging allows for the characterization of infarct-related injury and residual ischemia. A scenario-based imaging approach supports informed clinical decision-making in patients with MI.

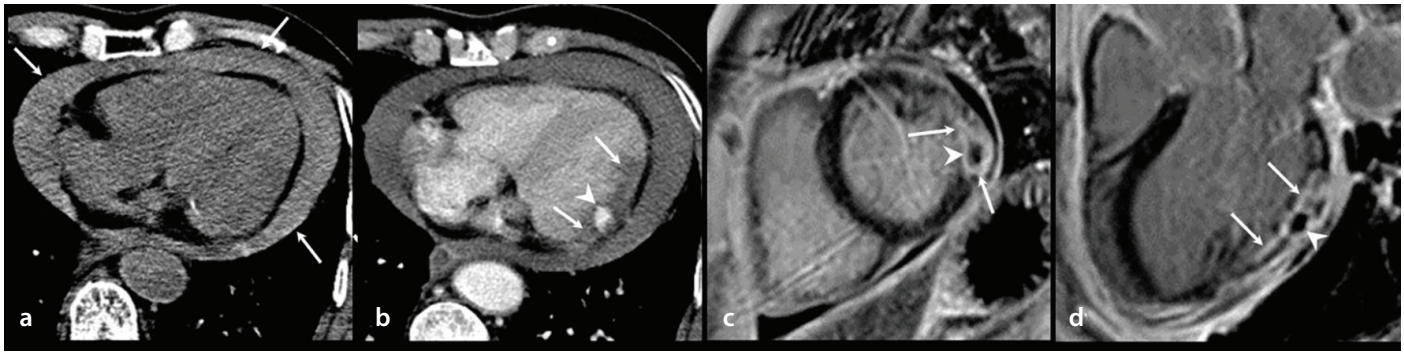

Figure 10. Post-MI LV free wall rupture in a 79-year-old man with NSTEMI. (**a**): Non-contrast axial CT image shows massive acute hemopericardium (arrows). (**b**): Contrast-enhanced axial CT image shows a patchy, contrast-filled outpouching lesion (arrowhead) in the lateral LV wall with poor enhancement (arrows). (**c, d**): Short-axis (**c**) and three-chamber (**d**) LGE-CMR images show transmural delayed enhancement (arrows) with central low signal intensity (arrowheads) in the basal to mid-lateral LV wall. Oval-shaped low signal intensity lesion was considered a thrombus within the ruptured LV wall. The patient underwent open-heart surgery, and an LV free wall rupture of the oozing type was noted in the inferolateral LV wall. NSTEMI, non-ST-segment elevation myocardial infarction; CT, computed tomography; LV, left ventricular; CMR, cardiac magnetic resonance; LGE, late gadolinium enhancement.

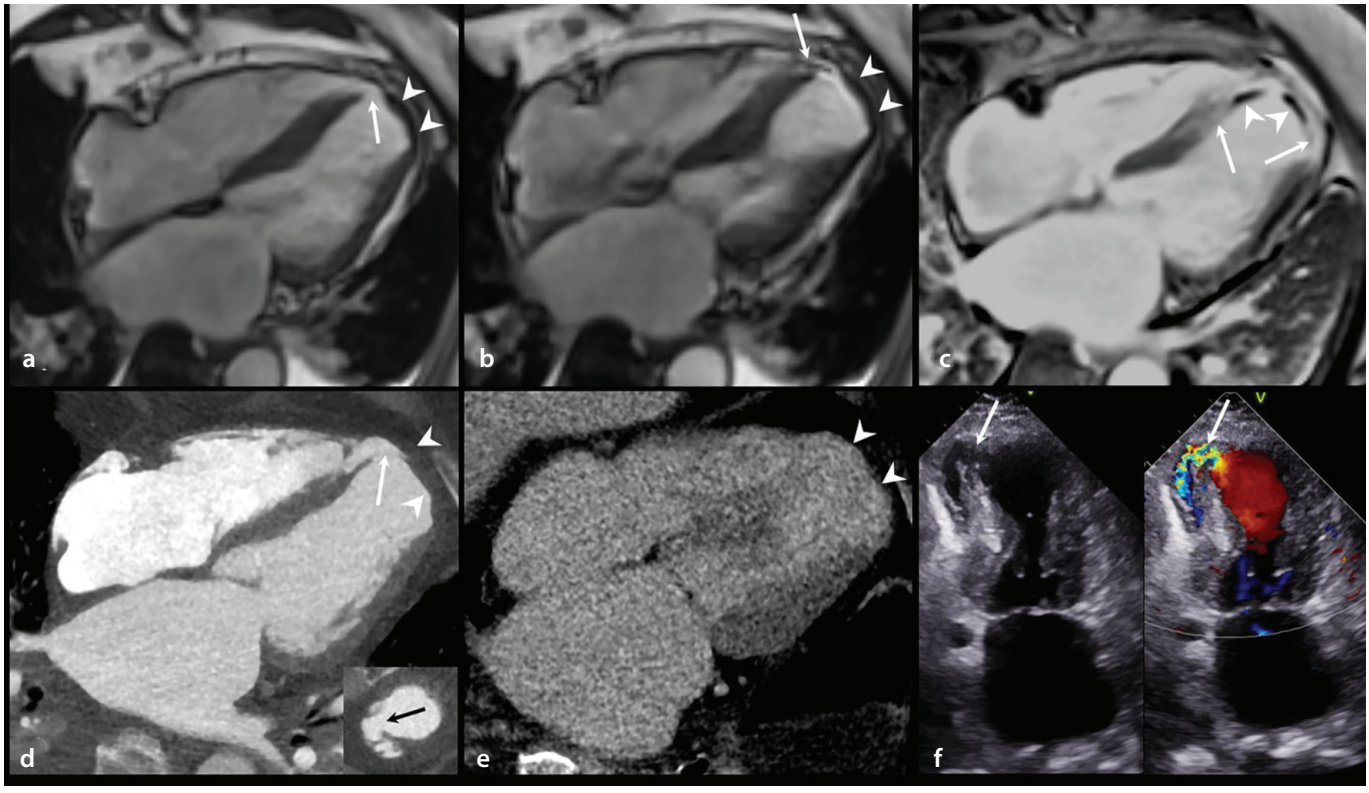

Figure 11. Post-MI LV septal rupture in an 80-year-old woman with STEMI. (**a, b**): Four-chamber cine CMR images in the end-diastolic (a) and end-systolic (**b**) phases demonstrate LV apical akinesia with increased wall thickness (arrowheads) and a pencil-like signal void (**b**, arrow) through a focal defect in the apical septum (**a**, arrow). (**c**): Four-chamber LGE-CMR image shows transmural delayed enhancement with patchy MVO (arrowheads) in the apex as well as in the apical septal and lateral and mid-septal LV walls (arrows). (**d, e**): Four-chamber MPR arterial phase (**d**) and delayed-phase (**e**) CT images show focal thinning with an apical septal defect (**d**, arrow) and increased wall thickness (**d**, arrowheads) of the apex and apical lateral LV walls with delayed hyperenhancement (e, arrowheads). (**f**): Apical four-chamber view of color Doppler echo images shows shunt flow through a focal defect in the apical septum (arrow). The patient underwent open-heart surgery, and a 3-cm defect was found in the lower part of the apical septum and sutured with a bovine patch. Apical aneurysmal change was removed and reinforced using felt material. STEMI, ST-segment elevation myocardial infarction; b-SSFP, balanced steady state-free precession; CMR, cardiac magnetic resonance; CT, computed tomography; LGE, late gadolinium enhancement; MPR, multiplanar reformation

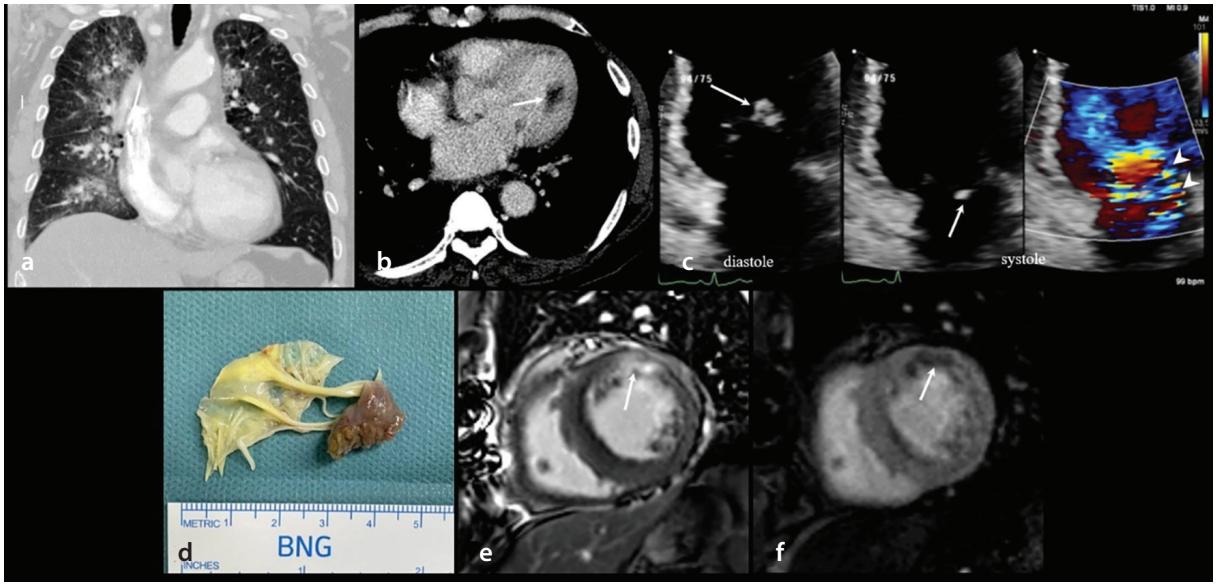

Figure 12. Acute severe MR resulting from papillary muscle rupture in a 68-year-old man who presented with sudden shortness of breath. (**a**): Coronal MPR image of a chest CT scan shows pulmonary edema in both lungs (primarily in the right lung). (**b**): Contrast-enhanced axial chest CT image shows hypoenhancement in the anterolateral papillary muscle (arrow). (**c**): Apical four-chamber view of color Doppler echo images shows severe eccentric MR (arrowheads) resulting from an anterolateral papillary muscle rupture (arrows) and associated mitral valve prolapse (mainly A2). The patient immediately underwent emergency surgery for mechanical mitral valve replacement, and an anterolateral papillary muscle rupture was discovered (**d**). Two weeks later, the patient underwent stress perfusion CMR imaging to evaluate the underlying cause of the anterolateral papillary muscle rupture. (**e, f**): LGE (**e**) and stress perfusion (**f**) CMR images show transmural delayed enhancement (**e**, arrow) and stress-induced, patchy transmural perfusion defects (**f**, arrow) in the mid-anterior and anterolateral LV segments. MR, mitral regurgitation; MPR, multiplanar reformation; CMR, cardiac magnetic resonance; CT, computed tomography; LGE, late gadolinium enhancement.

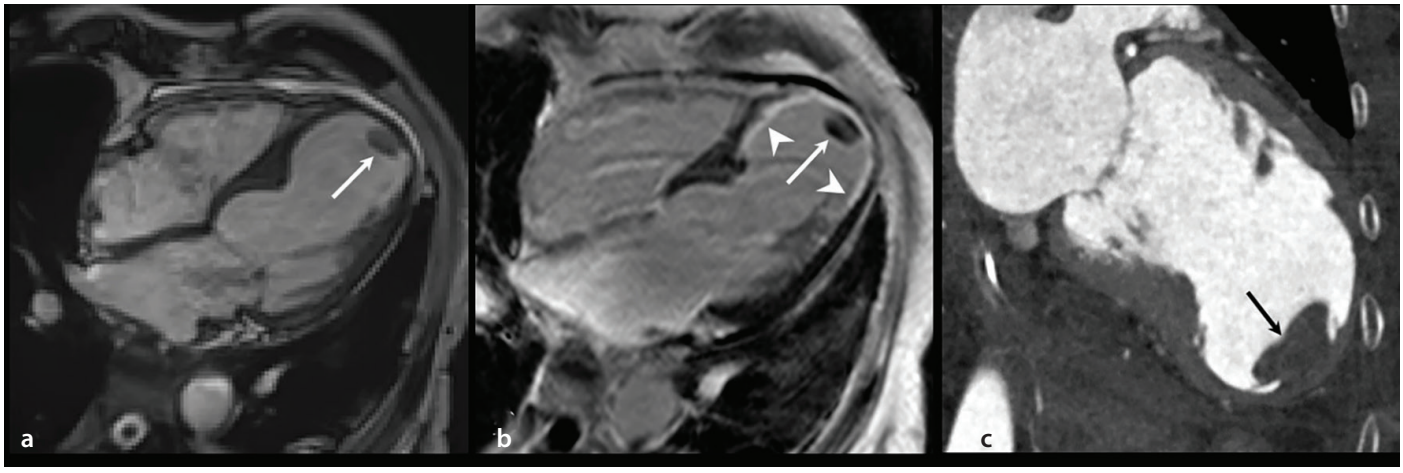

Figure 13. True LV aneurysm in a 75-year-old woman with a history of reperfused STEMI. (**a–c**): Four-chamber cine (**a**) and LGE-CMR images (**b**) and a two-chamber MPR CT image (**c**) show an apical aneurysm of the left ventricle with transmural delayed enhancement (**b**, arrowheads) and an apical thrombus (arrows). STEMI, ST-segment elevation myocardial infarction; LV, left ventricular; MPR, multiplanar reformation; CMR, cardiac magnetic resonance; CT, computed tomography; LGE, late gadolinium enhancement.

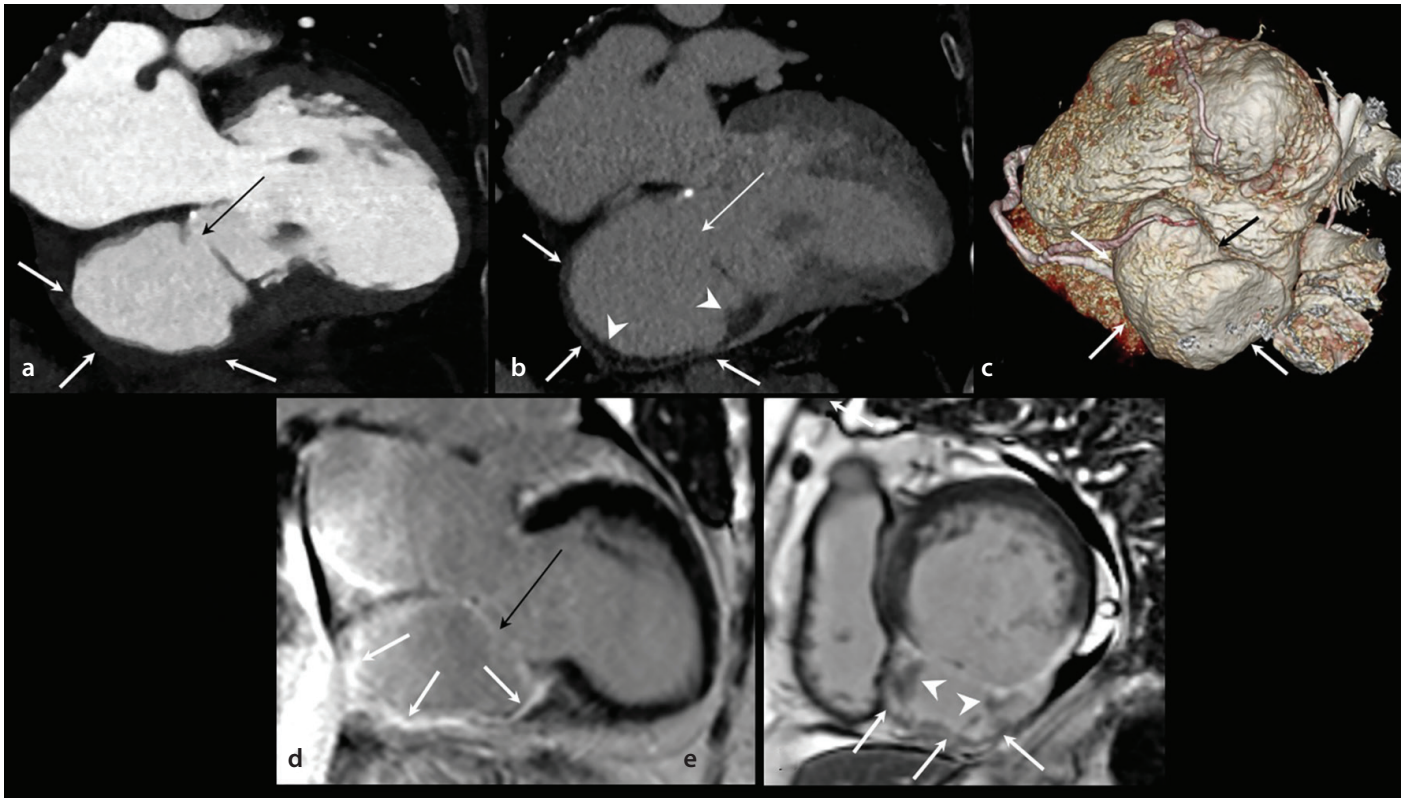

Figure 14. Left ventricular pseudoaneurysm in an 80-year-old woman with a history of reperfused STEMI. (**a, b**): Two-chamber MPR early contrast-enhanced (**a**) and MDE (**b**) CT images demonstrate a pseudoaneurysm of the basal to mid-inferior wall of the left ventricle with a narrow neck (long arrow), very thin wall (arrows), and intracavitary thrombus (arrowheads). (**c**): Three-dimensional, volume-rendering CT image of the heart shows a large aneurysm (arrows) arising from the inferior wall of the left ventricle. (**d, e**): Two-chamber (**d**) and short-axis (**e**) LGE-CMR images demonstrate a large inferior pseudoaneurysm with a narrow neck (**d**, long arrow), diffuse LGE of the pseudoaneurysm wall (arrows), and a thrombus (**e**, arrowheads). The surgical finding was consistent with a pseudoaneurysm caused by a rupture of the LV wall secondary to MI. STEMI, ST-segment elevation myocardial infarction; LV, left ventricular; MPR, multiplanar reformation; CMR, cardiac magnetic resonance; CT, computed tomography; LGE, late gadolinium enhancement; MDE, myocardial delayed enhancement.

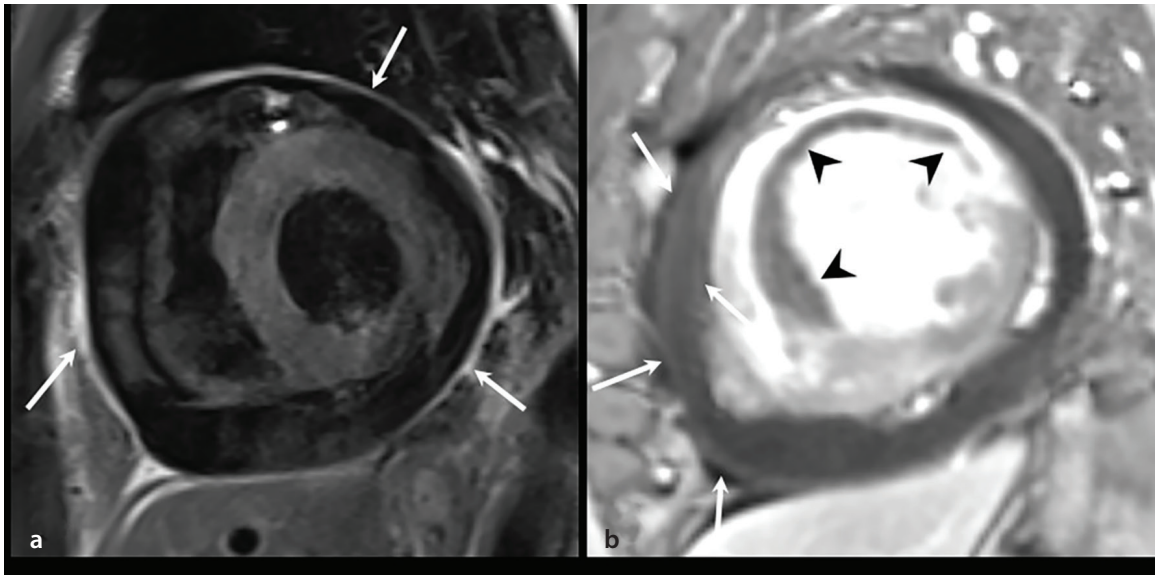

Figure 15. Post-MI pericarditis in a 62-year-old man with reperfused STEMI. (**a**): Short-axis T2-weighted STIR CMR image shows increased pericardial signal intensity (arrows) reflecting pericardial edema. A moderate amount of pericardial effusion is also seen. (**b**): Short-axis LGE-CMR image shows increased pericardial enhancement (arrows) suggestive of pericardial inflammation and extensive MVO (arrowheads) in the mid-anterior, anterolateral, and anteroseptal LV walls. STEMI, ST-segment elevation myocardial infarction; LGE, late gadolinium enhancement; STIR, short tau inversion recovery; CMR, cardiac magnetic resonance; LV, left ventricular; MVO, microvascular obstruction.

Table 1. Algorithm for clinical imaging modality selection following myocardial infarction

Clinical scenario	Preferred modality	Rationale
Hemodynamically unstable acute MI	Echocardiography	Bedside, real-time assessment of ventricular function and mechanical complications.
Post-reperfusion viability and area at risk	CMR imaging	Gold standard for assessing infarct size, transmurality, area at risk, and MVO.
Non-culprit lesion significance/residual ischemia	Stress CMR or cardiac CT (CCTA + CT-derived MPI/ CT-FFR)	Functional assessment of ischemia with an integrated anatomic–functional assessment.
Suspected LV thrombus	CMR (long-TI LGE) imaging	Highest diagnostic accuracy for thrombus detection and characterization.
MRI contraindicated	Cardiac CT (MDE-CT)	Complementary alternative for myocardial viability assessment.
Mechanical complications	CT + echocardiography + CMR	Comprehensive evaluation of anatomy, hemodynamics, and myocardial integrity.
Remodeling/prognosis	CMR (T1 mapping, ECV, MVO)	Quantitative biomarkers for risk stratification and outcome prediction.

MI, myocardial infarction; CMR, cardiac magnetic resonance; MVO, microvascular obstruction; CT, computed tomography; CCTA, coronary CT angiography; MPI, myocardial perfusion imaging; FFR, fractional flow reserve; LV, left ventricular; TI, inversion time; LGE, late gadolinium enhancement; MRI, magnetic resonance imaging; MDE, myocardial delayed enhancement; ECV, extracellular volume.

Footnotes

Conflict of interest disclosure

The authors declared no conflicts of interest.

Funding

This work was supported by the Natural Science Foundation of Shandong Province.

References

1. Salari N, Morddarvanjoghi F, Abdolmaleki A, et al. The global prevalence of myocardial infarction: a systematic review and meta-analysis. *BMC Cardiovasc Disord*. 2023;23(1):206. [Crossref]
2. Rajiah P, Desai MY, Kwon D, Flamm SD. MR imaging of myocardial infarction. *RadioGraphics*. 2013;33(5):1383-1412. [Crossref]
3. Peper J, Suchá D, Swaans M, Leiner T. Functional cardiac CT-going beyond anatomical evaluation of coronary artery disease with cine CT, CT-FFR, CT perfusion and machine learning. *Br J Radiol*. 2020;93(1113):20200349. [Crossref]
4. Williams MC, Weir-McCall JR, Baldassarre LA, et al. Artificial intelligence and machine learning for cardiovascular computed tomography (CCT): A White Paper of the Society of Cardiovascular Computed Tomography (SCCT). *J Cardiovasc Comput Tomogr*. 2024;18(6):519-532. [Crossref]
5. Thygesen K, Alpert JS, Jaffe AS, et al. Fourth universal definition of myocardial infarction (2018). *Circulation*. 2018;138(20):e618-e651. [Crossref]
6. Kloner RA. Stunned and hibernating myocardium: where are we nearly 4 decades later? *J Am Heart Assoc*. 2020;9(3):e015502. [Crossref]
7. Bulluck H, Dharmakumar R, Arai AE, Berry C, Hausenloy DJ. Cardiovascular magnetic resonance in acute ST-segment-elevation myocardial infarction: recent advances, controversies, and future directions. *Circulation*. 2018;137(18):1949-1964. [Crossref]
8. Liu D, Borlotti A, Viliani D, et al. CMR native T1 mapping allows differentiation of reversible

versus irreversible myocardial damage in ST-segment-elevation myocardial infarction: an OxAMI Study (Oxford Acute Myocardial Infarction). *Circ Cardiovasc Imaging*. 2017;10(8):e005986. [Crossref]

9. Chen Y, Ren D, Guan X, et al. Quantification of myocardial hemorrhage using T2* cardiovascular magnetic resonance at 1.5T with ex-vivo validation. *J Cardiovasc Magn Reson*. 2021;23(1):104. [Crossref]
10. Bulluck H, Carberry J, Carrick D, et al. A noncontrast CMR risk score for long-term risk stratification in reperfused ST-segment elevation myocardial infarction. *JACC Cardiovasc Imaging*. 2022;15(3):431-443. [Crossref]
11. Ma Q, Ma Y, Wang X, et al. A radiomic nomogram for prediction of major adverse cardiac events in ST-segment elevation myocardial infarction. *Eur Radiol*. 2021;31(2):1140-1150. [Crossref]
12. Garcia MJ, Kwong RY, Scherrer-Crosbie M, et al. State of the art: imaging for myocardial viability: a scientific statement from the American Heart Association. *Circ Cardiovasc Imaging*. 2020;13(7):e000053. [Crossref]
13. Nagel E, Greenwood JP, McCann GP, et al. Magnetic resonance perfusion or fractional flow reserve in coronary disease. *N Engl J Med*. 2019;380(25):2418-2428. [Crossref]
14. Alyousef T, Malhotra S, Iskander F, et al. Left ventricular intramyocardial dissecting hematoma: a multimodality imaging diagnostic approach. *Circ Cardiovasc Imaging*. 2021;14(7):e012410. [Crossref]
15. Pontone G, Baggiano A, Andreini D, et al. Stress computed tomography perfusion versus fractional flow reserve CT derived in suspected coronary artery disease: the PERFECTION Study. *JACC Cardiovasc Imaging*. 2019;12(8 Pt 1):1487-1497. [Crossref]
16. Dewey M, Siebes M, Kachelrieß M, et al. Clinical quantitative cardiac imaging for the assessment of myocardial ischaemia. *Nat Rev Cardiol*. 2020;17(7):427-450. [Crossref]
17. Rodriguez-Granillo GA. Delayed enhancement cardiac computed tomography for the assessment of myocardial infarction: from bench to bedside. *Cardiovasc Diagn Ther*. 2017;7(2):159-170. [Crossref]
18. Nishii T, Kobayashi T, Tanaka H, et al. Deep Learning-based post hoc CT denoising for myocardial delayed enhancement. *Radiology*. 2022;305(1):82-91. [Crossref]
19. Stephens NR, Restrepo CS, Saboo SS, Baxi AJ. Overview of complications of acute and chronic myocardial infarctions: revisiting pathogenesis and cross-sectional imaging. *Postgrad Med J*. 2019;95(1126):439-450. [Crossref]
20. Damluji AA, van Diepen S, Katz JN, et al. Mechanical complications of acute myocardial infarction: a scientific statement from the American Heart Association. *Circulation*. 2021;144(2):e16-e35. [Crossref]